ELSEVIER

PII: S0032-3861(97)00070-0

Polymer Vol. 38 No. 14, pp. 3713–3715, 1997

0032-3861/97/$17.00 + 0.00

The interfibrillar phase in poly(ethylene terephthalate) fibre

V. B. Gupta* and A. K. Jain†
Department of Textile Technology, Indian Institute of Technology, New Delhi-110 016, India

and A. V. Moharir and Nam Prakash
Nuclear Research Laboratory, Indian Agricultural Research Institute, New Delhi-110 012, India
(Received 16 December 1996)

Transmission electron microscopy (TEM) at high magnification of thin cross-sections of drawn multifilament poly (ethylene terephthalate) yarn and of this yarn after heat-setting in the slack state at 250°C and in the taut state at 258°C is shown to provide evidence for the existence of crystallites whose lateral dimensions are consistent with those measured from wide-angle X-ray diffraction (WAXD). The denser, crystalline microfibrils appear to be separated by interfibrillar material of lower density in all the samples examined. The electron micrographs bring out the important differences in the morphologies of the three samples, the implications of which are critically examined. © 1997 Elsevier Science Ltd.

(Keywords: poly (ethylene terephthalate); microfibril; interfibrillar phase)

Introduction

The microfibrillar model of fibre morphology, which is applicable to a number of drawn, oriented thermoplastic fibres including poly(ethylene terephthalate) PET fibre, envisages long and thin rod-like microfibrils as the basic elements of fibrous structure; the microfibrils themselves being built up from alternating crystalline and amorphous regions stacked vertically along the fibre axis. There is growing evidence for the presence of a significant amount of interfibrillar phase in these fibres which provides interlinkages between the fibrils[1–9]. The amorphous phase in fibres is composed of oriented and non-oriented components; the highly oriented mesophase was called the third phase by Lindner[10] and it was shown[10,11] that the fraction of this third phase decreases with increase in the temperature of heat treatment. It was also shown[11] that Hermans' amorphous orientation factor and the third phase are representative of the same parameter, i.e. orientation of the amorphous phase. It is generally believed that the oriented amorphous phase may be located both within and between the microfibrils though it has recently been suggested[5] that the amorphous phase is isotropic within the fibril. The extent of the interfibrillar phase has been evaluated through indirect methods based on the combined use of Takayanagi's model[12] with the sonic modulus data[13] or through a combination of the measured crystal length by WAXD and the long period by low angle X-ray diffraction[4,9]. The results of such measurements on a variety of PET fibres suggested that the interfibrillar phase formed zero to 50% of the total amorphous phase. Direct observation of thin transverse sections of oriented PET fibres prepared by heat-setting the drawn, oriented fibres for up to 3.70 s under variable tension at 225°C on an electron microscope[1], showed that a significant amount of interfibrillar phase was present and its electron density was higher than that of the neighbouring microfibril. This led to the formulation of a model of PET fibre with a highly oriented interfibrillar phase, which has been extensively quoted in the literature.

In the present investigation, an attempt was made to observe the microfibrils and the interfibrillar phase directly in three PET samples, viz. as-drawn PET fibre with low crystallinity and this fibre annealed for 5 min at 250°C in the slack condition and at 258°C in the taut state; both the annealed fibres used are highly crystalline. The amorphous phase was highly oriented in the as-drawn sample and was almost isotropic in the free-annealed sample with the taut-annealed sample having an intermediate degree of amorphous orientation. It was hoped that the widely varying morphologies of the three samples would provide useful information. The results of this study are reported in this communication.

Experimental

The starting material was conventional two stage PET yarn of 76 denier, 36 filaments and zero twist. It had been spun at 800 m min^{-1} and then drawn to a draw ratio of 3.92 at a wind-up speed of 642 m min^{-1}. This control sample was subjected to isothermal heat-setting in a silicone oil bath for 5 min at a temperature of 250°C while free to shrink (designated as free-annealed or FA 250) and at a temperature of 258°C while held taut at constant length (taut-annealed or TA 258).

For TEM, single filaments were carefully separated from the yarn and embedded in a low density resin ('Spurr') in such a manner that sections perpendicular to the fibre axis could be obtained. The embedded sample blocks were first trimmed and transverse sections about 500 Å thick were obtained with a freshly cut glass knife fitted to an ultramicrotome. In order to provide more support to the microtomed sections, copper grids were

* To whom correspondence should be addressed
† Present address: Indian Council of Agricultural Research, Krishi Bhavan, New Delhi-110 001, India

coated with a thin layer of evaporated carbon film before being used.

A Phillips EM300 TEM was used to examine these sections. Imaging was conducted under low illumination conditions with a small spot size with an accelerating voltage of 80 kV, the crystalline texture being preserved during the course of imaging.

In addition to examining a number of unstained sections, samples stained with 1% lead citrate and 2% uranyl acetate were also examined. The stain was, however, found to be ineffective for heat-set samples and the observation and analysis were therefore confined to micrographs obtained for the unstained sections. The crystal widths perpendicular to the fibre axis were measured for 100 crystals in each micrograph and the average of these measurements has been reported.

The X-ray diffraction (XRD) technique was also employed to measure (a) the crystal widths t_{010} and t_{100}, perpendicular to (0 1 0) and (1 0 0) planes, using the Scherrer equation, and (b) the crystalline fraction and crystallite orientation using standard procedures described elsewhere[14,15].

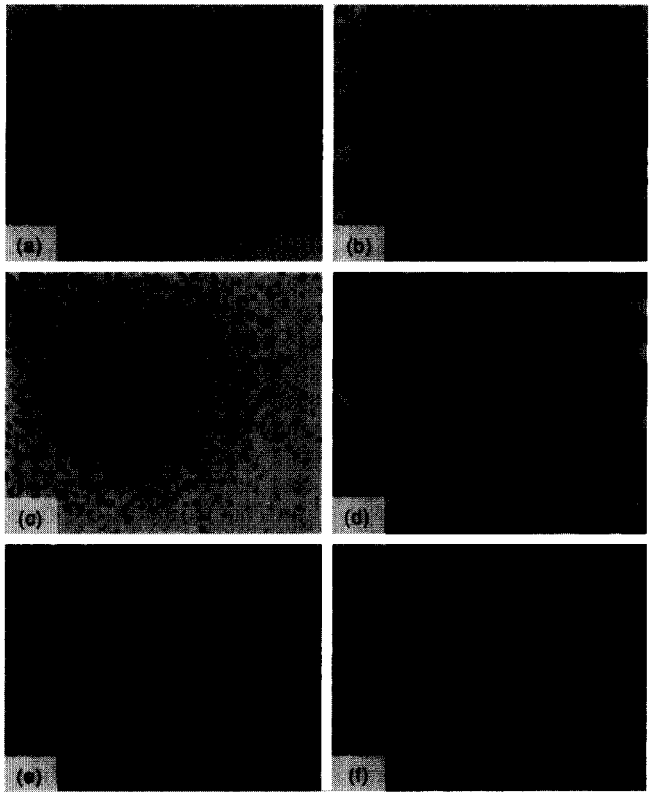

Figure 1 Transmission electron micrographs of the unstained thin transverse sections of PET fibre samples: (a) control (X 2,04,200); (b) control (X 6,12,600); (c) TA 258 (X 2,04,200); (d) TA 258 (X 6,12,600); (e) FA 250 (X 2,04,200); and (f) FA 250 (X 6,12,600)

The i.r. spectroscopic technique, as described elsewhere[16], was used to measure the amorphous orientation factor.

Results and discussion

The transmission electron micrographs of the unstained control, TA 258 and FA 250 samples are presented in *Figure 1*. The average widths of the dark spots, as obtained from 100 measurements on the electron micrographs, and the average lateral width of the crystal as determined from XRD studies by taking it as the arithmetical mean, $(t_{010} + t_{100})/2$, of the two measurements for the three samples are shown in *Table 1* along with other relevant structural data. It is noteworthy that these two different techniques give quite close values in all the three cases, thus indicating that the dark spots represent the microfibrils in the thin section examined. The surrounding area of light shade would then represent the scattered intensity from the interfibrillar phase. It may, however, be emphasized that this would be the case for an ideal situation in which the rod-like microfibrils are embedded in a matrix of amorphous material. This is rarely the case as the microfibrils in the fibre are not rod-like. Moreover, the thin section would not be expected to be exactly perpendicular to the fibre axis and may even be slightly uneven. It is, however, interesting to note that in spite of these limitations, the selected micrographs show quite sharp features, particularly in the heat-set samples. Some of the principal features of these micrographs will now be discussed.

The control sample (*Figures 1a* and *b*) contains the thinnest microfibrils and the amount of interfibrillar phase in this sample is relatively much larger than in the other two samples. Considering that the crystal size, as measured by XRD, and the degree of crystallinity of this sample are the smallest, this is an expected result. It may also be noted from *Table 1* that the amorphous orientation factor is the highest for this sample and this would imply that the molecules in the interfibrillar space would be highly oriented. The small crystallites in this sample have also been shown to be highly defective[17]. The identification of the dark spot with the microfibril will thus imply that the amorphous phase within the microfibril is also highly oriented and the microfibril is therefore more electron dense than the surrounding interfibrillar phase.

The microfibrils in the two heat-set samples are thicker than those in the control sample and their lateral dimension is slightly higher in the case of the FA 250 sample compared to the TA 258 sample, as is also revealed by XRD for the crystal widths. Another noteworthy feature is that the interfibrillar phase surrounding the microfibrils occupies a larger volume in the case of the FA 250 sample than in the TA 258 sample. Apparently this is because compared to slack

Table 1 Crystal size and other related data on the three PET fibre samples

	Crystal width (Å)					Orientation function	
	X-ray			TEM			
Sample	t_{100}	t_{010}	Average	Average	Crystalline fraction	Crystalline (X-ray)	Amorphous (i.r.)
Control	30.4	41.2	35.8	37.2	0.34	0.94	0.58
TA250	50.4	74.9	62.7	69.8	0.59	0.94	0.28
FA258	57.6	82.4	71.5	73.9	0.59	0.86	0.04

annealing, annealing with fixed ends does not allow the same freedom for structural reorganization. As a result, the sample annealed in the slack state at temperatures of 200°C and above shows larger absolute SAXS intensity and distinct phase separation[9]; both the factors being related to the electron density difference between the rather perfect crystals and the essentially random amorphous phase.

Another noteworthy observation is the fusion of crystallites in the TA 258 sample (*Figures 1c* and *d*). This apparently implies that the microfibrils may have fused at some points along their length. This is not surprising, for when the sample is held taut at constant length, the crystallites in adjacent fibrils can fuse together; a phenomenon unlikely to occur to the same extent in slack annealed sample which shrinks during annealing. Such a fusion of crystallites has been observed in PET films crystallized under high strain rates[18] and in polypropylene[19].

The studies reported in this communication show that PET fibres can have a wide spectrum of morphologies depending on the method adopted to produce them. Thus no single model can represent the structures and morphologies that characterize these fibres. It would appear from this limited investigation that in the as-drawn sample, oriented amorphous phase is present both within the fibrils and between the fibrils. The sample heat-set at 250°C or above shows significant difference depending on whether heat-setting is done in the slack state or at constant length. The slack annealed sample contains a significant amount of interfibrillar phase which is essentially random whereas in the taut-annealed sample, the amorphous phase is substantially oriented both in the fibril and between the fibrils.

As noted earlier, an interfibrillar phase higher in electron density than the microfibrils has been reported in the literature[1], a result contrary to the present finding. Since the starting sample and the heat-setting parameters like temperature, time and tension were different in the two investigations, the morphological parameters which affect electron density, such as degree of crystallinity, crystal defect density, crystal size, the nature of the amorphous phase, etc., will be expected to be different. An explanation of this discrepancy will have to await a complete characterization of these features.

References

1. Prevorsek, D. C., Tirpak, G. A., Harget, P. J. and Reimschuessel, A. C., *J. Macromol. Sci.–Phys.*, 1974, **B9**(4), 733.
2. Yakubi, K., Iwasaki, M. and Aoki, Y., *Text. Res. J.*, 1986, **56**, 41.
3. Oudet, Ch. and Bunsell, A. R., *J. Mater. Sci.*, 1987, **22**, 4292.
4. Rim, P. B. and Nelson, C. J., *J. Appl. Polym. Sci.*, 1991, **42**, 1807.
5. Fu, Y., Annis, B., Boller, A., Jin, Y. and Wunderlich, B. *J. Polym. Sci. Part B: Polym. Phys.*, 1994, **32**, 2289.
6. Chang, H., Lee, K. G. and Schultz, J. M., *J. Macromol. Sci.–Phys.*, 1994, **B33**(1), 105.
7. Ward, I. M., *J. Text. Inst.*, 1995, **86**, 289.
8. Gupta, V. B., *J. Text. Inst.*, 1995, **86**, 299.
9. Ramesh, C., Gupta, V. B. and Radhakrishanan, J., *J. Macromol. Sci.–Phys.* (in press).
10. Lindner, W. L., *Polymer*, 1973, **14**, 9.
11. Gupta, V. B. and Kumar, S., *Polymer*, 1978, **19**, 963.
12. Takayanagi, M., Imada, J. and Kajiyama, T., *J. Polym. Sci. Part C*, 1966, **15**, 263.
13. Gupta, V. B., Ramesh, C. and Gupta, A. K., *J. Appl. Polym. Sci.*, 1984, **29**, 3115.
14. Gupta, V. B. and Kumar, S., *J. Polym. Sci., Polym. Phys. Ed.*, 1979, **17**, 179.
15. Gupta, V. B. and Kumar, S., *J. Appl. Polym. Sci.*, 1981, **26**, 1865.
16. Jain, A. K. and Gupta, V. B., *J. Appl. Polym. Sci.*, 1990, **41**, 2931.
17. Gupta, V. B., Jain, A. K., Radhakrishnan, J. and Chidambareswaran, P. K., *J. Macromol. Sci.–Phys.*, 1994, **B33**(2), 185.
18. Petermann, J. and Rieck, U., *J. Polym. Sci.: Part B: Polym. Phys.*, 1987, **25**, 279.
19. Schultz, J. M. and Petermann, J., *J. Colloid Polym. Sci.*, 1984, **262**, 294.